
Figures and figure supplements

Characterization of tryptophan oxidation affecting D1 degradation by FtsH in the photosystem II quality control of chloroplasts

Yusuke Kato, Hiroshi Kuroda and Shin-Ichiro Ozawa *et al.*

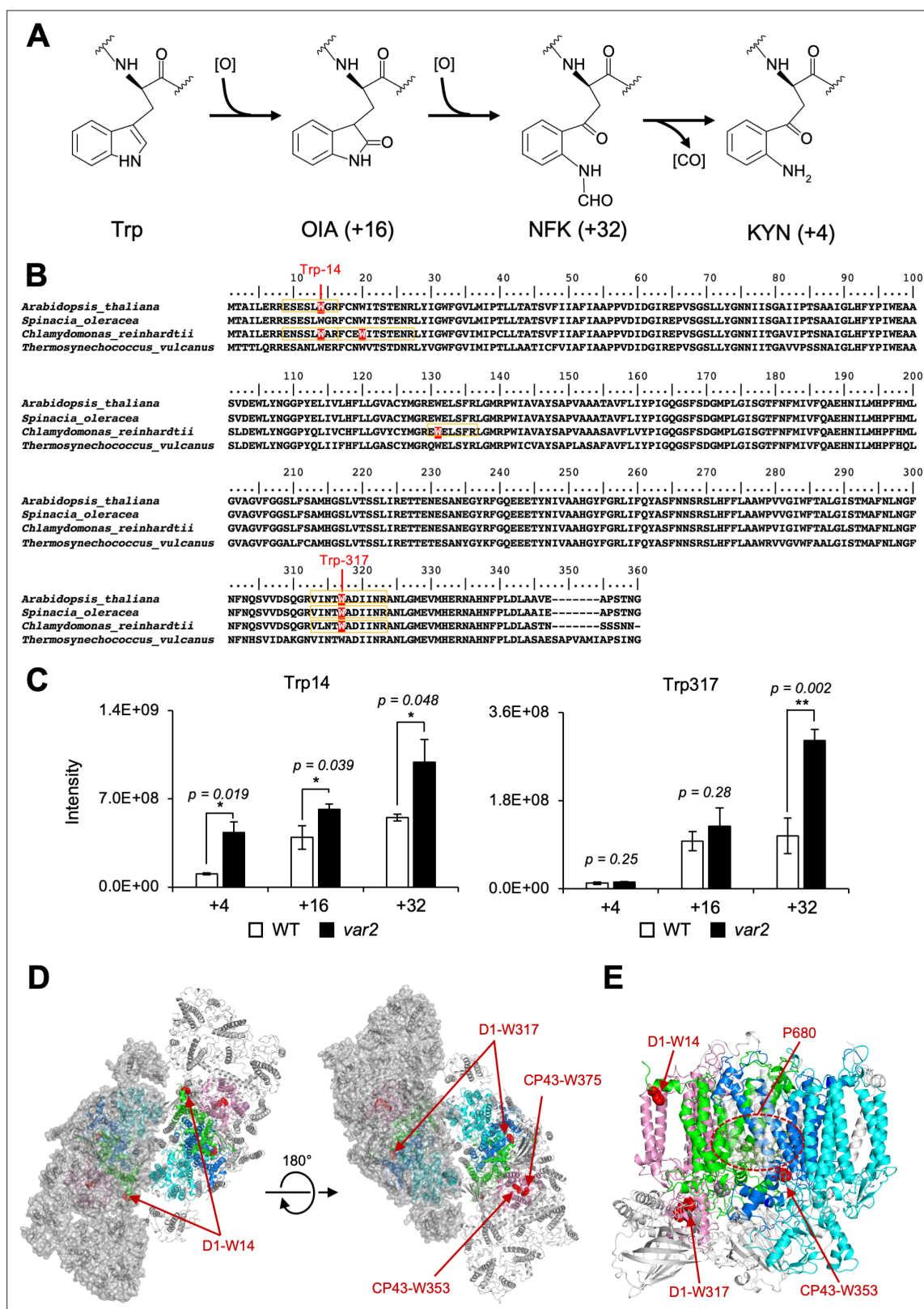


Figure 1. The Oxidized Trp residues in PSII complex. (A) Trp-oxidation pathway. OIA: oxindolylalanine, NFK: N-formylkynurenine, KYN: Kynurenine. (B) Multiple alignment of D1 protein from *Arabidopsis*, spinach, *Chlamydomonas*, and *Thermosynechococcus vulcanus*, showing oxidized Trp residues. Orange color boxes indicate the identified peptide by the MS-MS analysis. Oxidized Trp residues are highlighted in red. (C) Oxidation levels of three oxidative variants of Trp in Trp14 and Trp317 containing peptides in var2 and WT obtained by label-free MS analysis. The abundance of oxidized variants

Figure 1 continued on next page

Figure 1 continued

(+4: KYN, +16: OIA, and +32: NFK) of Trp14 and Trp317 were calculated using the intensity values. Asterisks indicate statistically significant differences between the mean values (* <0.05 , ** <0.01 ; Student's t-test). **(D–E)** Structural positions of oxidized Trp residues in PSII core proteins. The side chain of oxidized Trp residues are shown with red-colored space-filling model and indicated with arrows. The P680 special chlorophyll pair is indicated with dark-green colored ball-stick model in panel e. PSII dimer (panel d) and monomer (panel e) from *Chlamydomonas reinhardtii* (PDB ID is 6KAC) is shown in cartoon model without cofactors Top view from stromal side or lumenal side **(D)** and the side view from the dimer interface **(E)** are shown respectively. The color code of each subunit is, Green, D1; Dark blue, D2; Purple, CP43, Cyan, CP47. Protein structure graphics were generated with PyMOL ver. 2.4.0 software.

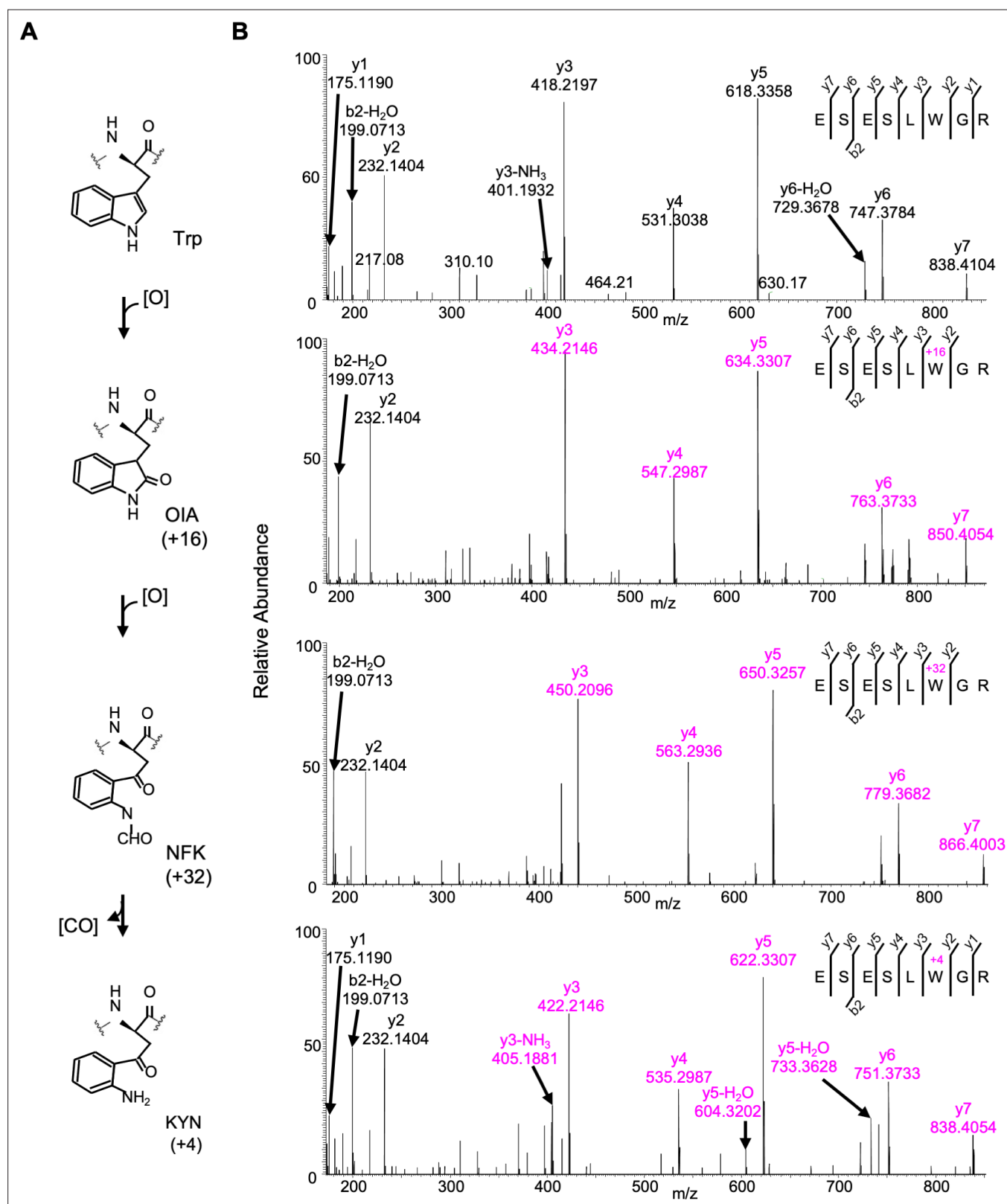


Figure 1—figure supplement 1. Detected oxidative modifications at Trp14 of D1 in *Arabidopsis thaliana*. (A) Trp-oxidation pathway. (B) Mass spectra of Trp14 carrying peptide ⁹ESEL(W)GR¹⁶ of D1 protein in *var2*. This oxidation led to the formation of oxindolylalanine (OIA), N-formylkynurenine (NFK), and kynurenine (KYN) with +16, +32, and +4 mass shifts, respectively.

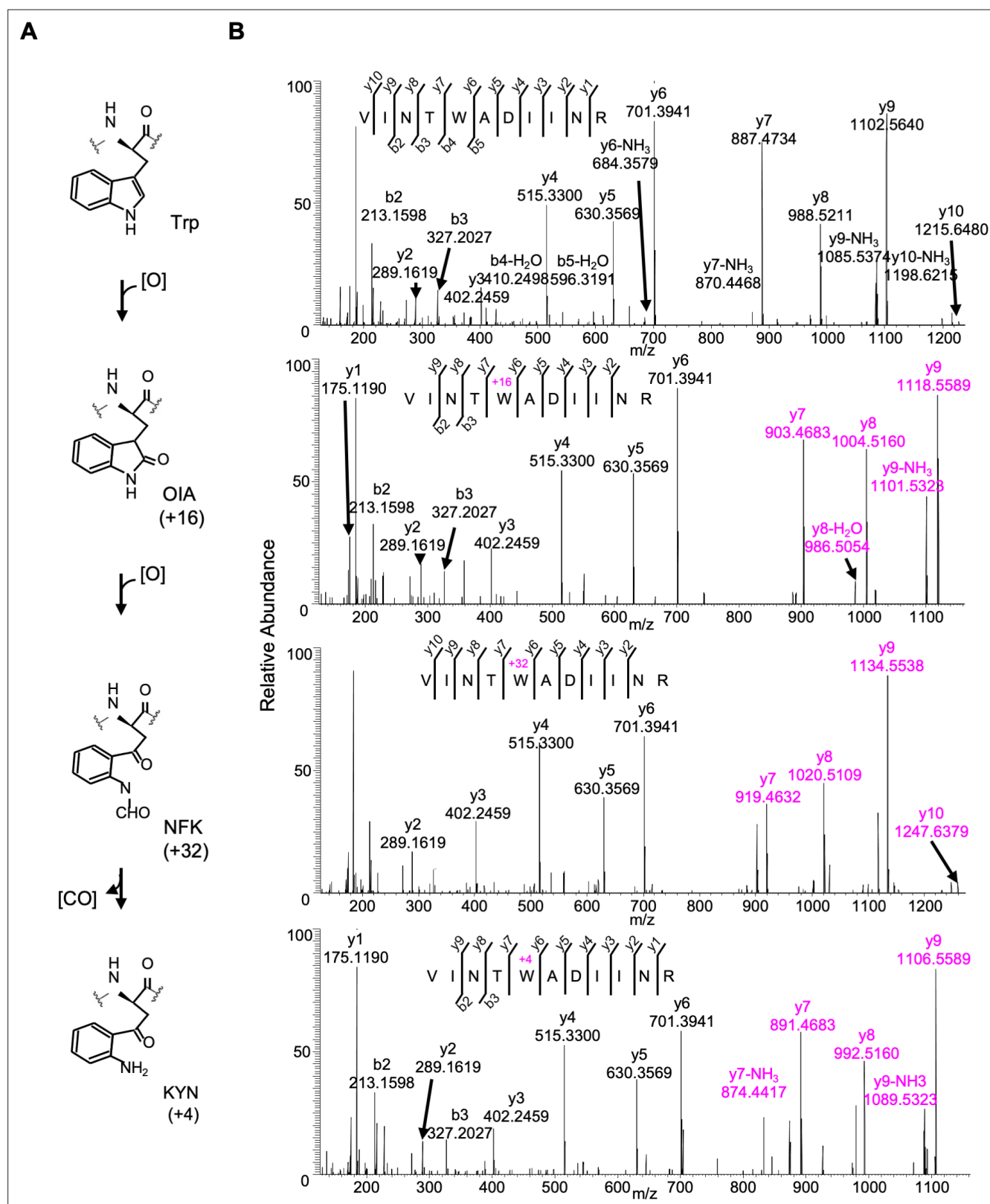


Figure 1—figure supplement 2. Detected oxidative modifications at Trp317 of D1 in *Arabidopsis thaliana*. **(A)** Trp-oxidation pathway. **(B)** Mass spectra of Trp317 carrying peptide $^{313}\text{VINT(W)ADIINR}^{323}$ of D1 protein in var2. This oxidation led to the formation of oxindolylalanine (OIA), N-formylkynurenine (NFK), and kynurenine (KYN) with +16, +32, and +4 mass shifts, respectively.

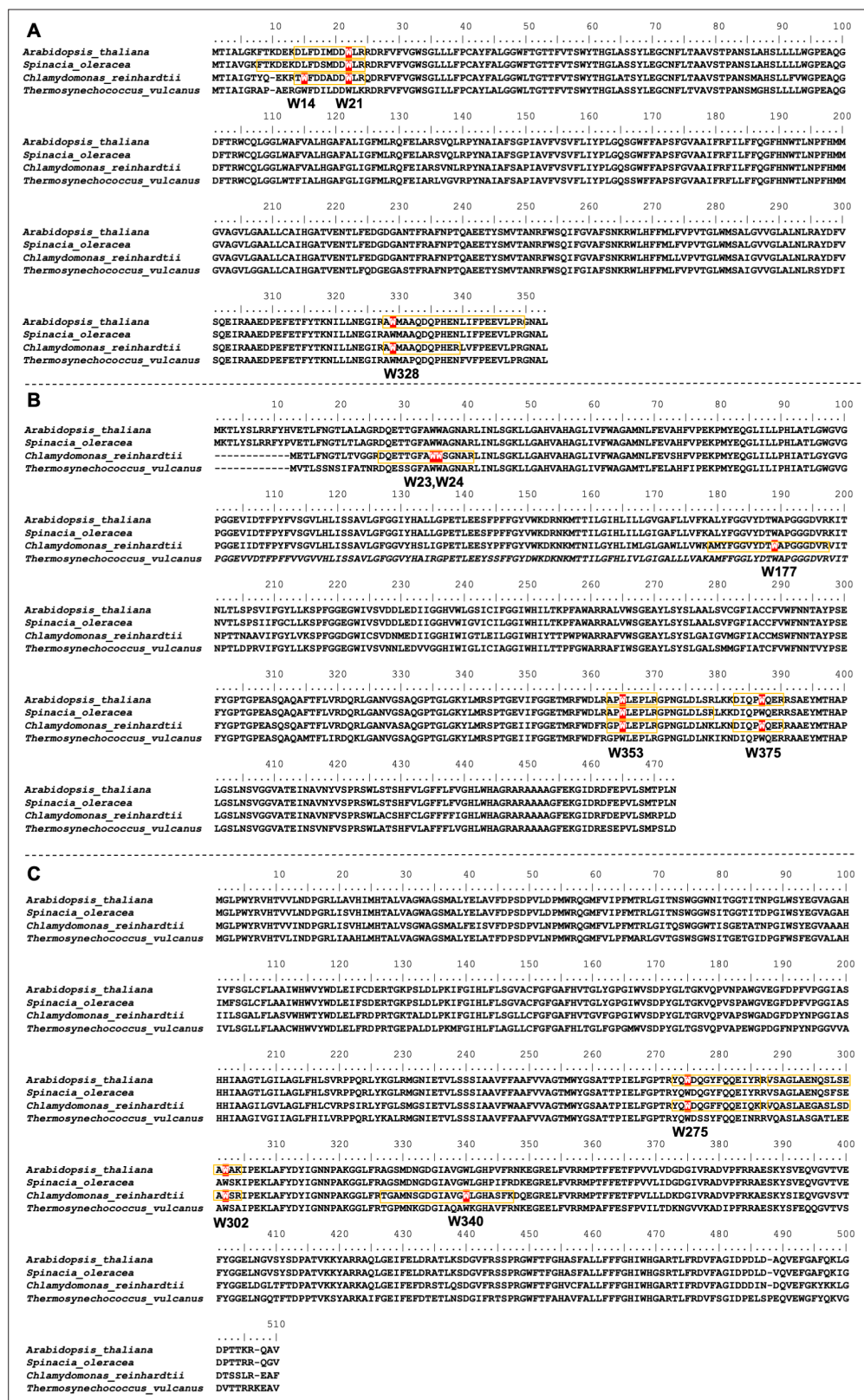


Figure 1—figure supplement 3. Positions of oxidized Trp residues in the identified peptide of PSII core complex by the MS-MS analysis. The oxidized Trp residues in D2 (A), CP43(B), and CP47 (C) were highlighted. Orange color boxes indicate the identified peptide by the MS-MS analysis. Oxidized Trp residues are highlighted in red.

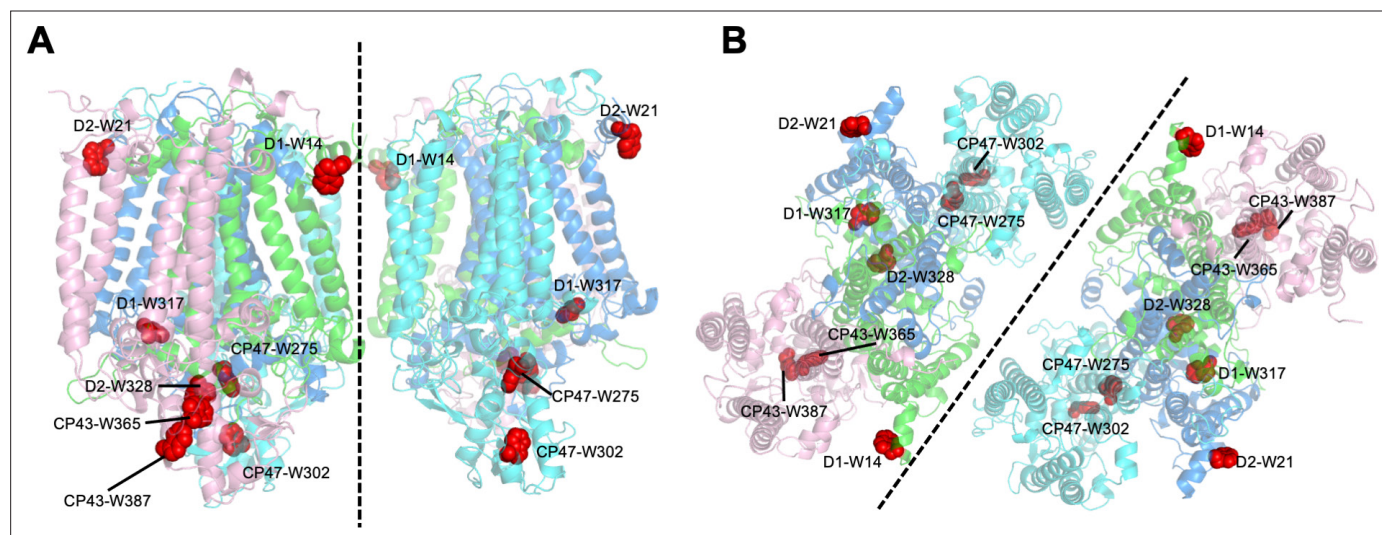


Figure 1—figure supplement 4. Structural positions of oxidized Trp residues in PSII core proteins. The structure is from *Thermosynechococcus vulcanus* (PDB id is 3WU2) and shown in cartoon model without cofactors by PyMOL ver. 2.4.0. The four PSII core subunits are colored in green (D1), marine blue (D2), pink (CP43), and cyan (CP47). The oxidized Trp residues are indicated by red. Side view (a) and top view (b) of the structure are respectively shown. Green, D1; Dark blue, D2; Purple, CP43, Cyan, CP47.

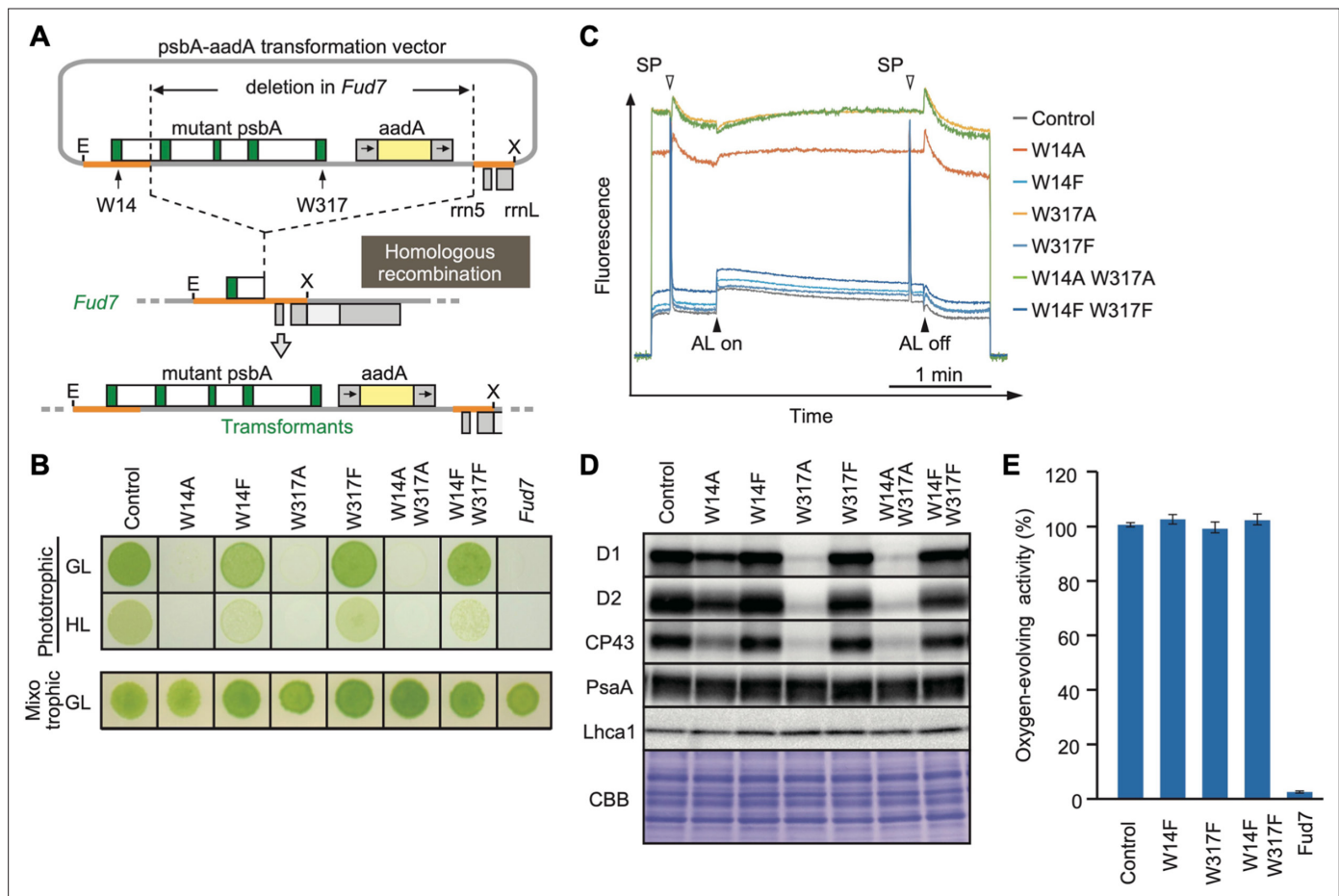


Figure 2. High-light sensitive phenotype in the *Chlamydomonas* D1 transformants in which Trp-14 and Trp317 were mutated. **(A)** Schematic drawing of the transforming vector carrying *psbA*, its flanking regions of the chloroplast DNA, and the selectable *aadA* marker cassette. E and X represent restriction sites of *EcoRI* and *XhoI*, respectively. Green boxes represent exons 1–5 of *psbA*. *Fud7* is the *psbA* deletion mutant of *Chlamydomonas*. **(B)** Phototrophic growth of Trp-substituted transformants on HSM medium and mixotrophic growth on TAP medium. GL, growth light (30 $\mu\text{mol photons m}^{-2}\text{s}^{-1}$); HL, high light (320 $\mu\text{mol photons m}^{-2}\text{s}^{-1}$). **(C)** Chlorophyll fluorescence induction kinetics in Trp-substituted transformants. SP, saturating pulse. AL, actinic light. **(D)** Protein accumulation in the transformants. Thylakoid proteins of cells grown in TAP medium under growth-light condition were separated by SDS-PAGE and analyzed by immunoblotting with antibodies against PSII subunits (D1, D2, and CP43), PSI subunits (PsaA), and light-harvesting complex of PSI (Lhca1). **(E)** Oxygen-evolving activity of the transformants.

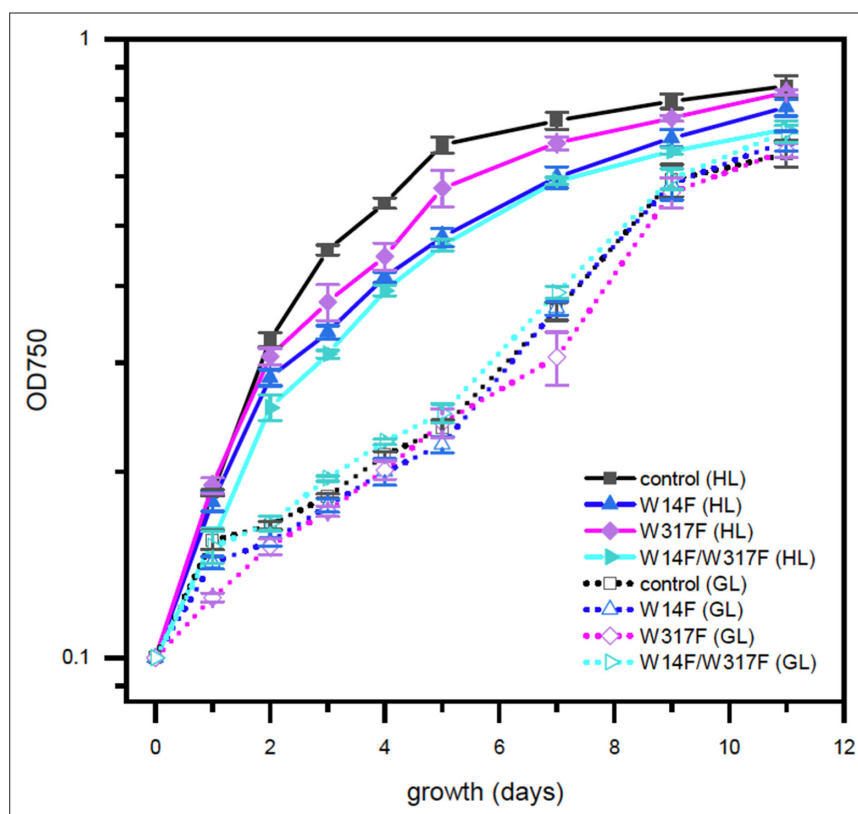


Figure 2—figure supplement 1. High-light sensitive phenotype in the *Chlamydomonas* D1 transformants in which Trp-14 and Trp317 were mutated. Phototrophic growth of Trp-substituted transformants on HSM medium. GL, growth light ($30 \mu\text{mol photons m}^{-2}\text{s}^{-1}$); HL, high light ($320 \mu\text{mol photons m}^{-2}\text{s}^{-1}$).

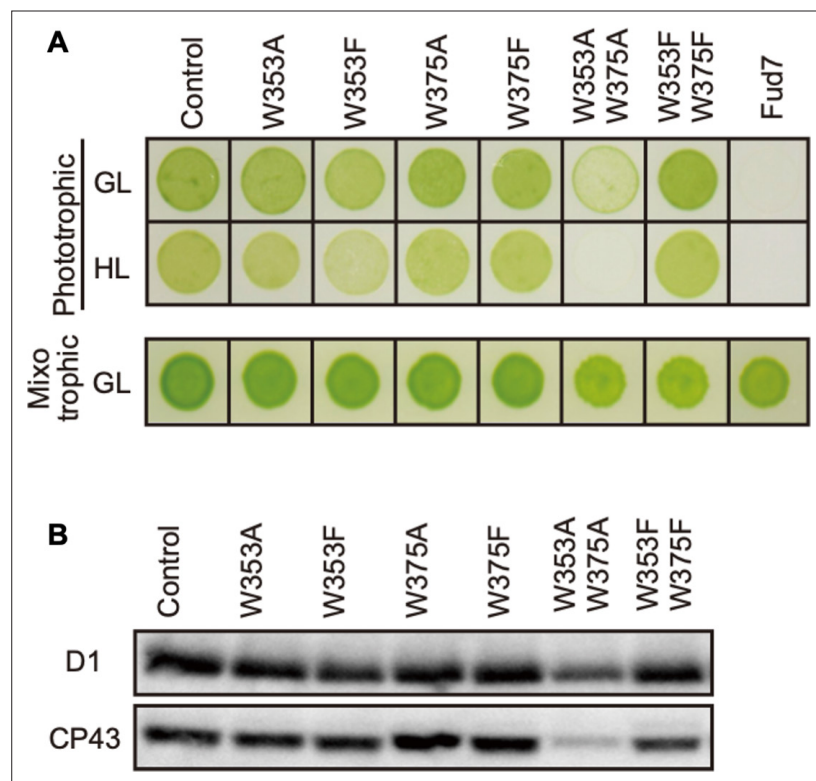


Figure 3. Characterization of *Chlamydomonas* CP43 transformants in which Trp-353 and Trp-375 were mutated. **(A)** Phototrophic growth on HSM medium and mixotrophic growth on TAP medium at growth light (GL) at $30 \mu\text{mol m}^{-2}\text{s}^{-1}$ or high light, (HL) at $320 \mu\text{mol m}^{-2}\text{s}^{-1}$. **(B)** Protein accumulation in the transformants. Thylakoid proteins of cells grown in TAP medium under growth light condition were separated by SDS-PAGE and analyzed by immunoblotting with antibodies against PSII subunits (**D1** and **CP43**).

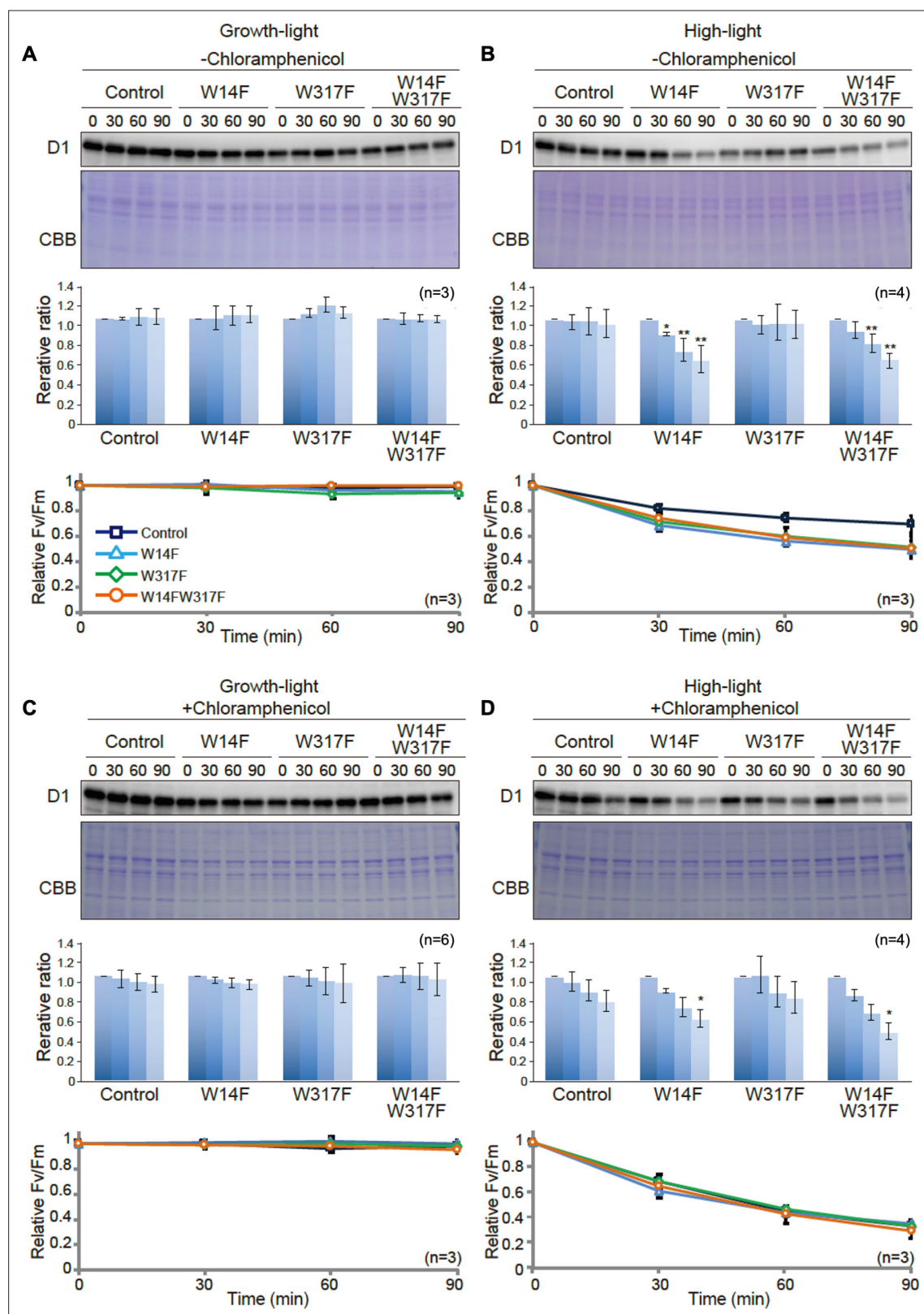


Figure 4. D1 degradation assay in W14F and W317F transformants demonstrating enhanced D1 degradation under high-light stress. The transformants were incubated under high-light ($320 \mu\text{mol photons m}^{-2}\text{s}^{-1}$) or growth-light ($30 \mu\text{mol photons m}^{-2}\text{s}^{-1}$) conditions in the absence or presence of inhibitor of chloroplast protein synthesis, CAM, and subjected to D1 degradation assay. (A) Growth-light in the absence of CAM; (B) high-light in the absence of CAM; (C) growth-light in the presence of CAM; (D) high-light in the presence of CAM. Immunoblot results of D1 in the transformants are shown at the

Figure 4 continued on next page

Figure 4 continued

top of each panel. A representative immunoblot using anti-D1 is depicted. Quantified D1 levels using NIH Image program are shown in the middle. Values are means \pm SD. Asterisks indicate statistically significant differences between the mean values (* <0.05 , ** <0.01 ; Student's t-test). Time course analysis of maximal photochemical efficiency of PSII, F_v/F_m , are shown at the bottom.

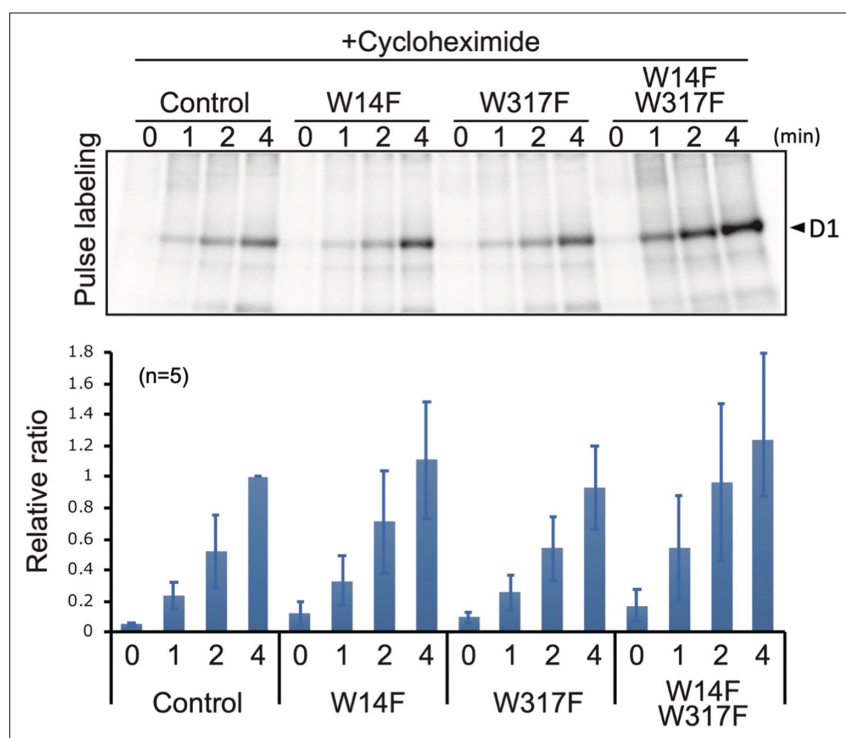


Figure 5. Protein synthesis in the transformants studied by in vivo protein labeling. Cells were radio-labeled in vivo with ^{35}S , in the presence of cycloheximide for 1, 2, and 4 min. Total proteins were separated by SDS-PAGE. The bands corresponding to D1 is indicated by arrowheads. Quantified newly synthesized D1 levels using the Image J program are shown in bottom panels. To normalize values from four independent experiments, the ratio of control at 4 min was adjusted as 1, and the relative ratios are indicated. Values are means \pm SD.

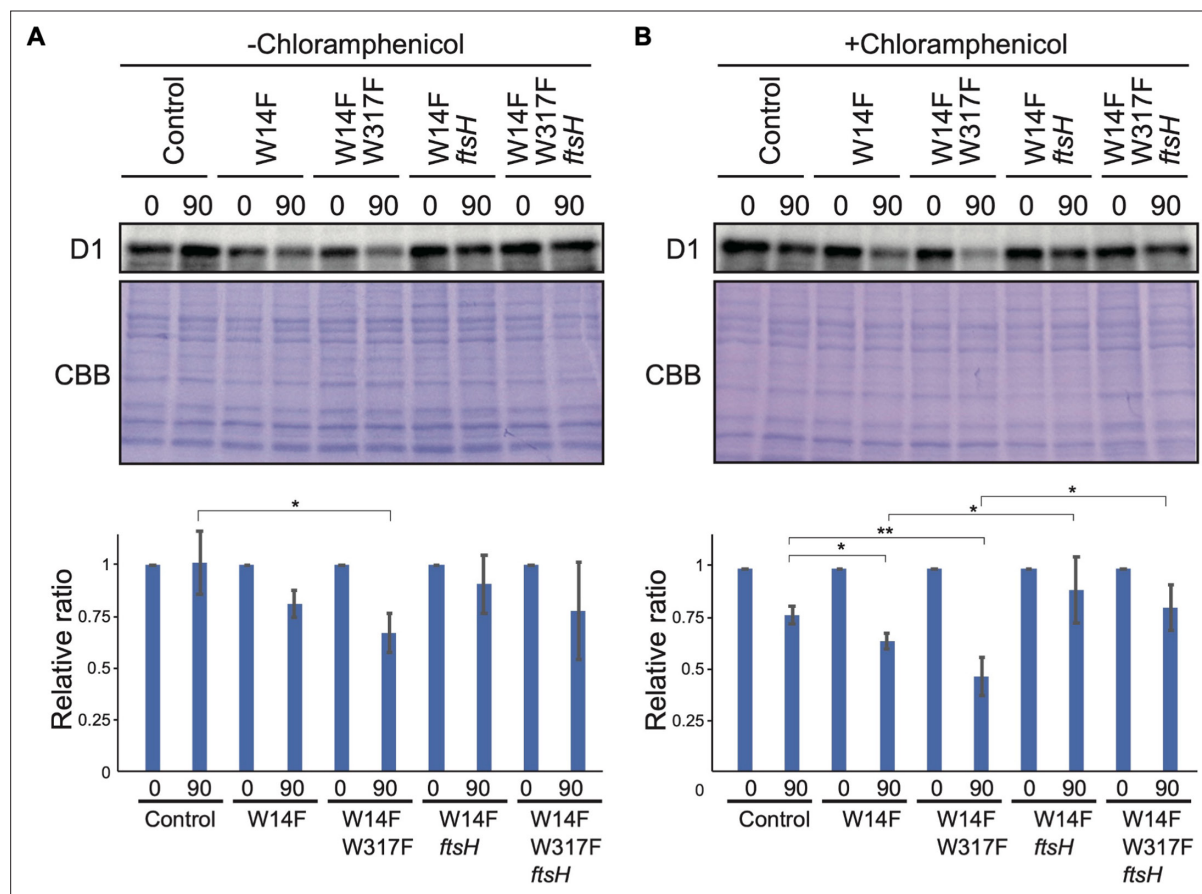


Figure 6. D1 degradation assay in W14F and W14F/W317F transformants in the *ftsH* mutant background. Rate of D1 degradation in the W14F *ftsH* and W14F/W317F *ftsH* was investigated as shown in **Figure 3**. Cultured cells were incubated under high-light conditions ($320 \mu\text{mol photons m}^{-2}\text{s}^{-1}$) in the absence (**A**) or presence (**B**) of CAM. Signals of immunoblots were quantified using NIH Image program. Values are means \pm SD ($n=4$). A representative immunoblot using anti-D1 is depicted. Values are means \pm SD. Asterisks indicate statistically significant differences between the mean values (* <0.05 , ** <0.01 ; Student's t-test).

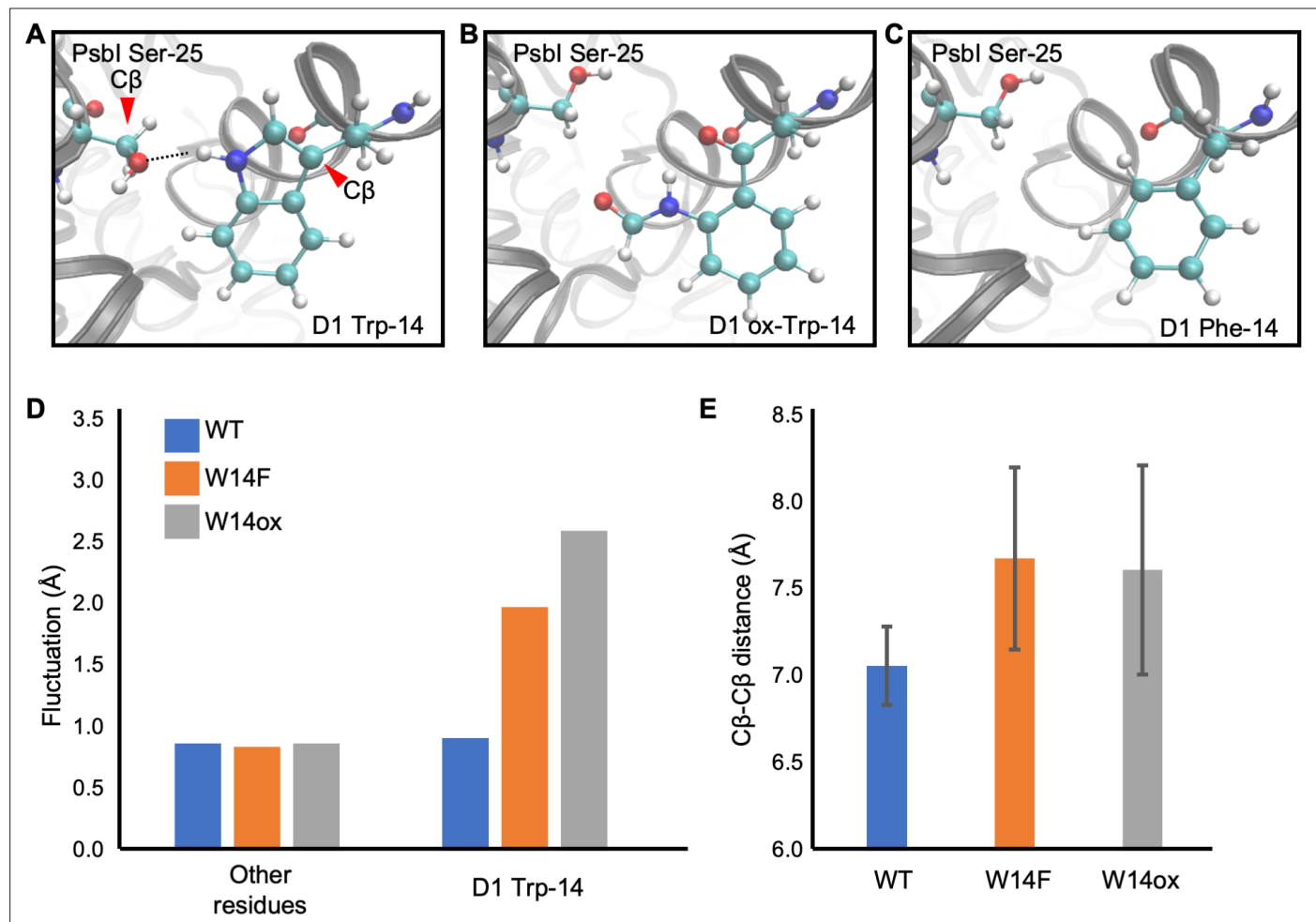


Figure 7. Snapshots and structural fluctuation of D1-Trp14 in molecular dynamics simulations of PSII. **(A)** The interaction between D1 Trp-14 and PsbI Ser-25. Dash line indicates the hydrogen bond between the side chains. **(B)** Position change of side-chain when D1 Trp-14 is oxidized to N-formylkynurenine. **(C)** Position change of side-chain when D1 Trp-14 is substituted to Phe. **(D)** The fluctuation of atoms at D1 Trp-14 in the MD simulation. **(E)** Averaged C β -C β distance between side chains of D1 Trp-14 and PsbI Ser-25. The error bars represent the standard deviations of the distances. The C β atoms are indicated as red arrowheads in **A**.

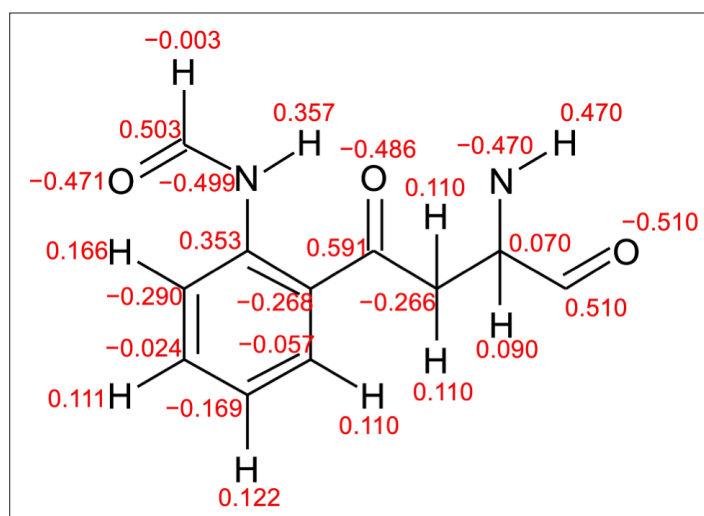


Figure 7—figure supplement 1. Atomic partial charges of NFK. Red values represent atomic partial charges calculated by using the RESP procedure.

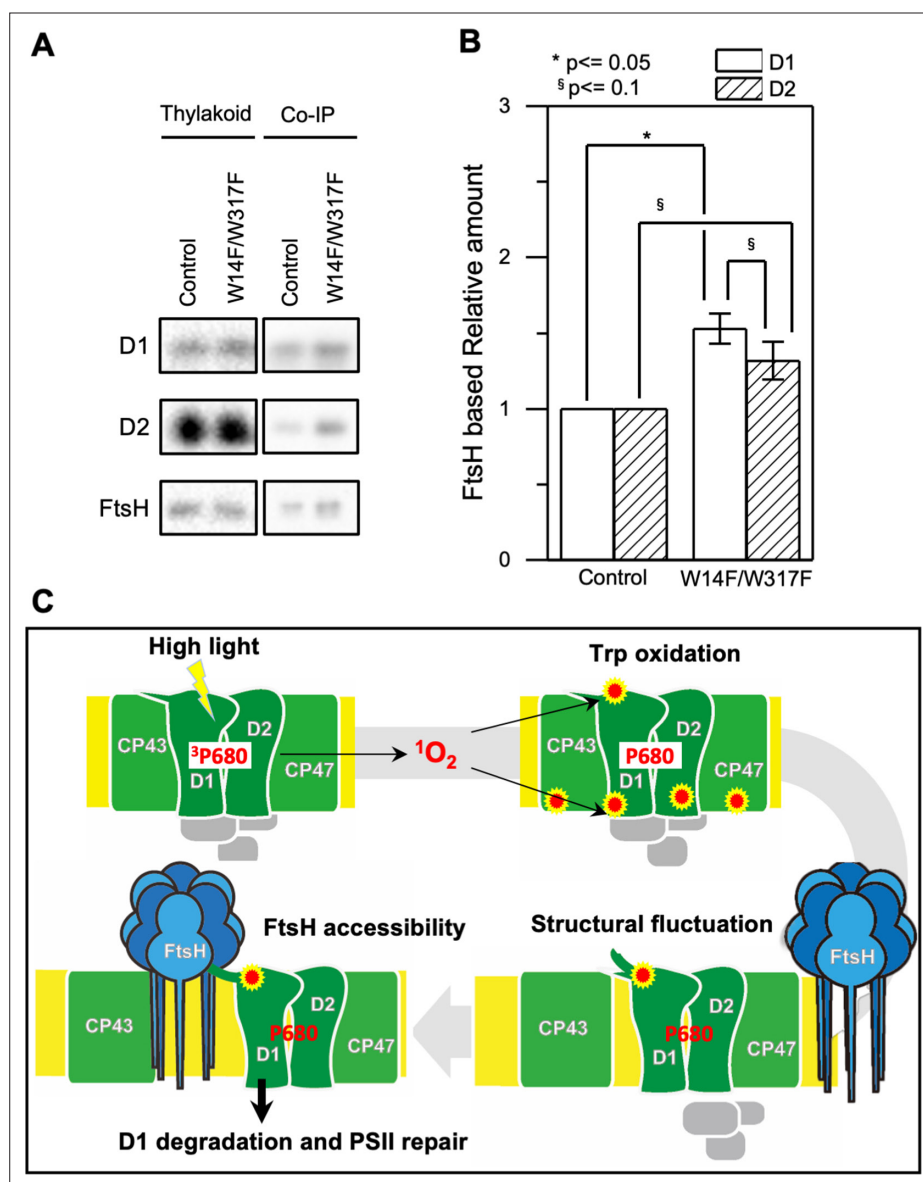


Figure 8. Augmented affinity of FtsH with D1 by W14F/W317F. **(A)** Coimmunoprecipitation was performed with anti-FtsH antibody using the thylakoid membrane isolated from control or D1-W14F/W317F. The polypeptides of thylakoid membrane or coimmunoprecipitated samples were separated by SDS-PAGE and detected by immunoblotting with anti-D1, anti-D2, and anti-FtsH antibody. **(B)** The immunoblotting signals are quantified and the ratio of D1 or D2 to FtsH are calculated. The averaged value and standard error for three biological replicates are shown. Significant difference was calculated by t-test and 0.1 (§) or 0.05 (*) probability confidence were indicated respectively. **(C)** A proposed model of photodamaged D1 recognition, in which Trp oxidation plays a role in recruiting FtsH. FtsH heterocomplexes (blue) and PSII core proteins (green) along with oxygen evolving protein complex (gray) in the thylakoid membrane are schematically shown. Trp-oxidized residues (red) are localized at both luminal and stromal sides. Trp-14 located at the N-terminus alpha helix enhances association of FtsH, whose catalytic site faces stroma.